Small Modular Reactor-based solutions to enhance grid reliability: impact of modularization of large power plants on frequency stability

Charly Boudot, Jean-Baptiste Droin, Pierre Sciora, Yvon Besanger, Bruno Robisson, Anne-Laure Mazauric

EPJ Nuclear Sci. Technol. **8**, 16 (2022)

https://doi.org/10.1051/epjn/2022015

EPJ Nuclear Sciences & Technologies

Available online at:
https://www.epj-n.org

Fuel Cycle Simulation TWoFCS 2021, Fanny Courtin, Francisco Alvarez-Velarde, Philippe Moisy and Léa Tillard (Guest editors)

REGULAR ARTICLE

OPEN ACCESS

Small Modular Reactor-based solutions to enhance grid reliability: impact of modularization of large power plants on frequency stability

Charly Boudot[1,2]*, Jean-Baptiste Droin[1], Pierre Sciora[1], Yvon Besanger[2], Bruno Robisson[3], Anne-Laure Mazauric[1,2]

[1] CEA, IRESNE, DES, DER, 13108 Saint Paul lez Durance, France
[2] Univ. Grenoble Alpes, CNRS, Grenoble INP*, G2Elab, 38000 Grenoble, France
[3] CEA, DRT, LITEN, DTS, 13108 Saint Paul lez Durance, France

Received: 15 July 2021 / Received in final form: 16 June 2022 / Accepted: 19 July 2022

Abstract. In the current renewable energies' expansion framework, the increasing part of intermittent electricity production sources (solar or wind farms) in the energy mix and the reducing part of thermal power stations that are nowadays useful to ensure grid stability will lead to a complete paradigm shift concerning the means to ensure grid stability. Nuclear energy, which is carbon-free and dispatchable, may be a sustainable solution to this grid reliability issue if it is adequately designed and implemented on the grid. Several solutions aiming at improving the future nuclear power flexibility are currently under investigation in the literature, among them are those based on Small Modular Reactor (SMR) plants. In order to demonstrate their potential ability to stabilize electric grids, it is necessary to perform electrical dynamic simulations taking into account a spatial and temporal discretization of the grid. In this paper, such calculations are performed using the PowerFactory software. This tool can reproduce electrical grids thanks to models of turbo generators, lines, transformers, loads, I&C systems, etc. The objective is to assess to what extent the innovative SMR features may enhance the frequency control of a grid. For this purpose, a short-circuit event and three frequency stability criteria are firstly defined. Then, a verification of the correct behaviour of the IEEE 39-bus (or New England) grid with regulations is carried out. The relevance of implementing Small Modular Reactors (SMR) instead of large power plants on such frequency stability criteria on this grid is finally assessed, in order to conclude in a preliminary way the possible contribution of small reactors to the future grid's sustainability.

1 Introduction

1.1 Context

The current energy policies are following the objective, among others, todrastically reduce greenhouse gas emissions at an international scale for environmental issues. In most of the cases, these strategies are based, on the one hand, on the reduction of the part of dispatchable fossil fuel power plants in the energy mix because of their high CO_2 emission rate for electric production. On the other hand, an increasing part of Variable Renewable Energies (VREs) is expected to compensate for the fossil fuel plants' installed capacity reduction. These expectations may derive in a complete paradigm shift concerning the grid stability control at a continental scale. Indeed, due to the expected fossil plants drastic reduction, the transmission and distribution system operators might need new means to control the overall electric production in order to ensure grid stability and reliability at different time scales.

Several technical solutions are currently studied [1] to bring answers to this need for power control levers. Regarding power sources, many studies are for instance devoted to power electronics as a means to deliver an accurate regulation of electronic parameters (current, voltage, power) for VREs. Also, forecast improvements based on artificial intelligence may increase the possibilities to predict – and thus control – this electricity production management. Increasing interconnection with neighbouring systems would also provide additional flexibility. Regarding the consumer, a demand-side management democratization might also improve the use and efficiency of energy production facilities.

As a complement to these potential levers aiming at stabilizing the next decades' grids, this paper is questioning the relevance of a nuclear-based solution to enhance

* e-mail: charly.boudot@cea.fr
* Institute of Engineering Univ. Grenoble Alpes

grid reliability for short time scales. Indeed, nuclear energy sources, that are carbon-free and easily dispatchable, might compensate for the fossil fuel plant drastic reduction if they are demonstrated to be flexible enough to accommodate increased power fluctuations on the grid [2]. In particular, the international R&D is nowadays very active on the Small Modular Reactor (SMR) topic because of their potential interest in economic [3] and safety issues [4] and, in the scope of this paper, for their potential increased contribution to grid stability relative to higher power plants.

For instance, [5] highlights the benefits of SMRs for frequency control in microgrids as well as some key issues related to their unit sizing, control and operation or interaction with other energy sources. It is shown in this paper that their easier association with secondary applications (district heating, desalination, etc.) than large nuclear power plants is a good opportunity to ensure effective frequency regulation. Furthermore, [6] proposes a model of hybrid SMR/thermal heating plant connected to a distribution network that can also be considered as a microgrid (105 MW of loads). The conclusion is that such hybrid plants can provide frequency regulation services, and even more efficiently with the help of batteries. In addition, [7] introduces a model of multi-module SMRs designed for frequency control and shows that the model system keeps electrical and thermodynamic variables well regulated during frequency-regulation operations. This argues in favour of the consideration that SMRs are a credible option for the electrical grid frequency control. Focusing on safety and flexibility issues, [8] eventually proposes a neutronic modelling of a passive SMR supplying frequency regulation and concludes that, for the SMR presented in this study, passive frequency control is technically feasible without exceeding the fuel thermo-mechanics safety criteria.

1.2 Small Modular Reactors and operational flexibility

Concerning this grid stability item, it is admitted by the IAEA that small- and medium-sized or modular reactors are an option to fulfil the need for flexible power generation for a wide range of applications [9]. Among them, SMRs deployable either as a single or multi-module plant, offer the possibility to combine efficiently nuclear with alternative energy sources, including renewables as mentioned in [10]. In its report [4], the IEA also argues that it should be recommended to accelerate innovation in new reactor designs, such as SMRs, that improve the operating flexibility of nuclear power plants to facilitate the integration of growing wind and solar capacity into the electricity system.

On a technical point of view, it seems that SMRs are better equipped than large power plants for an increased operational flexibility for several reasons (non-exhaustive list, mostly issued from [10]):

- the small power output means SMR units can support small grids with modest power demand or reinforce large grids by, for example, replacing ageing fossil fired power plants, which are typically small power sources themselves;
- with regard to operational flexibility at the plant level, power capacity can be scaled. In situations where small incremental additions are needed to satisfy slow growth in load demand, an SMR plant is a credible option;
- the reduced source term and relatively low thermal output of an individual SMR unit expand the options for siting, which enable closer positioning regarding power customers, or even co-location with heat processes and a reduction in the required water to support waste heat rejection;
- the inherent self-regulation and resilience to external events (e.g. station blackout, loss of heat sink...) possible for many SMR design concepts can substantially contribute to grid stability;
- SMRs can offer enhanced availability (i.e. increased capacity factors) through an extended operation cycle (i.e. significantly longer intervals between refuelling outages);
- in addition to the more traditional electric power role of nuclear power plants, non-electrical product streams can be supported by SMRs (district heating, desalination, hydrogen production...). It might then be possible to transition SMR output among multiple hybrid energy product streams depending on the demand (e.g. electricity production at peak demand times transitioning to other heat process at low demand times). This allows large electric power variations without affecting the SMR core thermal power that is kept constant during load following;
- finally, advanced SMRs may include design specificities such as innovative fuel elements (accident tolerant fuels) or innovative reactivity power control (boron-free designs) that may reduce the core solicitations during load following and thus increase the achievable core power ramps.

1.3 Objective of the study

This paper is therefore questioning the relevance of such a strategy based on SMRs to control the frequency of an incoming electrical grid. More specifically, it firstly aims to quantify the influence of their potential homogeneous distribution on the grid and of their expected higher flexibility degree on the short-time scale frequency evolution following an unpredicted event. This will be assessed in a preliminary way through the modularization (meaning the replacement by SMRs) of current large power plants (∼1 GW) towards SMR plants (∼250 MW) on a benchmark network named IEEE New-England 39-bus grid [11–13], representing the New England region.

2 Main assumptions

2.1 Software used

All calculations are performed with the PowerFactory 2020 software developed by DIgSILENT. This software

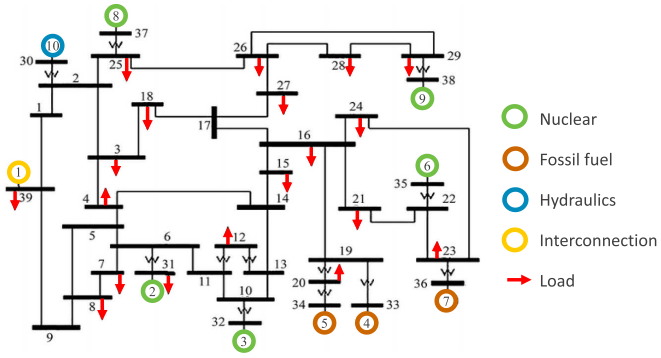

Fig. 1. Representation of the 39-bus grid with all generators surrounded by colour circles [20].

provides an environment with several models and automatic controls, to design, calculate and analyse electrical networks. The main modules that are used are the Load Flow module providing a steady-state calculation of the power flow in the network and the RMS (Root Mean Square) module providing dynamic simulations [14].

2.2 Electrical grid considered

The network considered for this preliminary study is the 39-bus grid [11,12] from IEEE [13] (Fig. 1). It represents a simplified version of the transmission electrical grid of the New England region in the USA. The nominal frequency is 60 Hz and the nominal voltage is 345 kV. Generator 1 is the interconnection with the rest of the USA and Canada. Generators 2, 3, 6, 8 and 9 are nuclear power plants. Generators 4, 5 and 7 are fossil fuel power plants and generator 10 is a hydraulic power station. The total installed capacity is 6800 MVA + 10000 MVA of interconnection (see Appendix A).

2.3 Machine modelling

Machines are described by a sixth-order dynamic model. This model with synchronous/transient/subtransient inductances and transient/subtransient time constants derives from a Park transformation of rotor and stator circuits of three-phase synchronous machines. This is the most common model used for dynamical simulation [15]. For more information about the calculation of both the transformations, and to this model in general refer to [15,16].

All values describing the 10 machines come from the IEEE benchmark and are referenced in Appendix A.

2.4 Reactor and regulation modelling

The dynamical response of the circuits upstream the turbine (including the core and the primary circuit) are not modelled in PowerFactory. The power response from the core and transmitted to the turbine is an input data, and it is considered to have the same kinetics for an SMR than for a large power plant. This is justified by safety issues: the maximal power ramp on the fuel element is constant independently from the design and the power level. The overall primary circuit thermal inertia is considered proportional to the power level for this preliminary study.

Regarding the Power Conversion System, all generators are equipped with classical control loops: a turbine-governor model (gov), an Automatic Voltage Regulator (AVR) and a Power System Stabilizer (PSS). The first one corresponds to the turbine modelling and control, meaning the power coming into the turbine and thus to the active power/frequency. The second one corresponds to the reactive power/voltage control, and the third one to the low frequency power oscillation damping.

2.5 Time scale and considered event

As a reminder, the electrical grid stability relies on:

- the angular stability: ability of all synchronous machines to synchronize themselves;
- the frequency stability: the synchronous frequency should not deviate too much from the nominal frequency value;
- the voltage values: the voltages on the whole grid should be maintained close to their nominal reference values.

We firstly focus on the frequency stability, voltage and angular stabilities being perspectives to this work. The time scale of interest is linked to the primary control of frequency, in other words from 10^{-1} to 10^{2} s. Short-circuits last less than one second, but their consequences in terms of frequency evolution last during several seconds. They are thus relevant events for the preliminary study described in this paper. However, the study of other events more representative of frequency regulation transients (load increase or decrease, intermittency on renewable energy production, etc.) is foreseen to confirm the robustness of the results described in this paper.

The considered event in the part 4 of this paper is a fugitive three-phase short-circuit on bus 16 with a resistive impedance of 1.19 Ω. This event is adapted from the ones proposed in a benchmark from the IEEE PES Task Force [13].

2.6 Preliminary validation

To ensure that the modelling of the 39-bus grid is correct and gives consistent results, a comparison with the benchmark [13] is carried out. This benchmark compares the load-flow, dynamical results and small-signal stability results obtained on a single grid (New England) with three different tools (one Matlab-based software, the ANAREDE/PacDyn/Anatem software package and the EMTP-RV software). The comparison with the Matlab-based software results is considered in this paper for validation purpose because the description of its results and assumptions is the most exhaustive. More details about

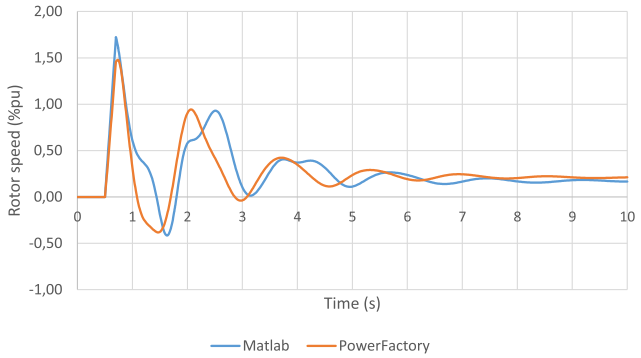

Fig. 2. Evolution of the rotor speed of generator 4 from Matlab IEEE-Benchmark and PowerFactory.

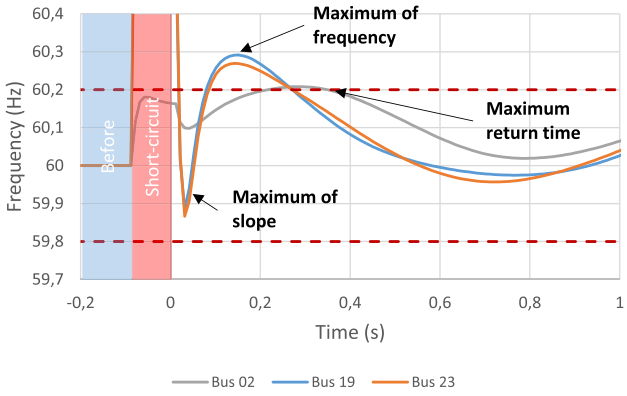

Fig. 3. Illustration of the way to assess the three estimators considered in this paper.

this Matlab modelling are available in [13]. The results of the load flow (i.e. the steady-state values characterizing the electrical flow network) confirm the good values of power repartition and impedance values. Indeed, the differences between the Matlab results from the benchmark and the ones obtained with PowerFactory are almost zero (see Appendix B).

The results displayed in Figure 2 show the evolution of the rotor speed in percent per unit of generator 4 (arbitrarily) from PowerFactory and from the Matlab part of the benchmark. For the comparison with the Matlab report of the IEEE benchmark [13], part 2.6 considers a fault duration of 200 ms.

A lack of comprehensive information provided in the benchmark does not allow us to lead a more precise work of validation. Indeed, the three reports do not consider exactly the same events for the dynamical simulation comparisons. For what concerns the short-circuit case, some features are missing to perform a complete validation exercise, such as the effective short-circuit impedance value. However, as a first approach, it confirms that the trends computed by the two tools are in good agreement.

From now on, it is considered that the fault is self-eliminated after 100 ms.

3 Analysis of a typical short-circuit event on the 39-bus grid

3.1 Definition of relevant estimators

To analyse how the frequency stability of the 39-bus grid evolves after a short-circuit, three estimators are considered. Note that all the nodes from 30 to 39 are excluded from the analyses because they correspond to the buses connecting the machines to their transformers, so they are inside the power plants and thus are not considered as grid buses. For each node from 1 to 29, the maximum frequency at the first swing following the frequency dip of the short-circuit is calculated. Then, those 29 maximum values are compared to keep only the maximum of them, which is then called "Maximum frequency". Similarly, the "Maximum frequency slope" and the "Maximum return time" to come back to a band of ±0.2 Hz (arbitrarily) around the nominal frequency are defined.

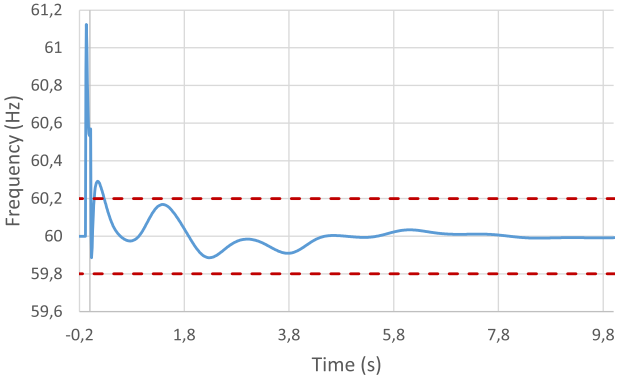

Fig. 4. Evolution of the frequency on bus 19, before, during and after a short-circuit.

The analysis of the frequency stability of a grid by studying the extreme values of frequency-related quantities had already been met in [17].

Figure 3 illustrates how the maximum frequency, maximum frequency slope and maximum return time for buses 2, 19 and 23 are calculated (time origin is also the end of short-circuit).

3.2 Transient analysis

Figure 4 shows the evolution of frequency at bus 19 (that is the bus from which comes the "maximum frequency" estimator, see Fig. 3) after the 100 ms and 1.19 Ω fault (the time origin corresponds to the end of the short-circuit).

Before the short-circuit, the network is stable with a 60 Hz frequency. When the short-circuit occurs at bus 16, a part of the power on the whole network goes to the short-circuit, which leads to a frequency increase as analysed in part 3.3. During the whole transient, regulations allow to adapt the power production to the power consumption, progressively bringing the frequency back to its nominal value. Figure 5 shows for instance the evolution of the turbine power with and without governor model regulation.

3.3 Physical analysis

The equation of motion (also called swing equation) [15] of a rotor is:

$$J\frac{\mathrm{d}\Omega}{\mathrm{d}t} = \Gamma_\mathrm{m} - \Gamma_\mathrm{e} \quad (1)$$

with

- J the moment of inertia of generator and turbine (in kg. m^2)
- Ω the mechanical rotating speed (in rad. s^{-1})
- Γ_m the motor torque called mechanical torque (in N. m) provided by the turbine to the generator and
- Γ_e the resistive torque called electrical torque (in N. m) coming from the load powers, including losses of the grid.

In our case, when the short-circuit occurs, the electrical power called by the network suddenly decreases due to the induced voltage drops at load buses, which means that the resistive torque on the rotor falls. Then, $\mathrm{d}\Omega/\mathrm{d}t$ becomes positive, leading to the acceleration of the alternator. This explains why the frequency on the grid increases during the short-circuit. When the short-circuit is over, all the power accumulated in the form of kinetic energy is restored to the grid, causing a frequency decrease and then oscillations around nominal frequency. If the short-circuit is too long, it may cause a loss of synchronism [15]. This is to avoid such complications that we chose a fugitive short-circuit limited to 100 ms instead of a 200 ms one as referenced in [13]. Furthermore, the natural behaviour of generators is also assisted by control loops (stated previously gov, AVR and PSS, respectively) that have the role to limit the consequences of an event by adjusting, for instance, the entry of power in the turbine, by adjusting reactive power or by smoothing inter-generator oscillations that can occurs.

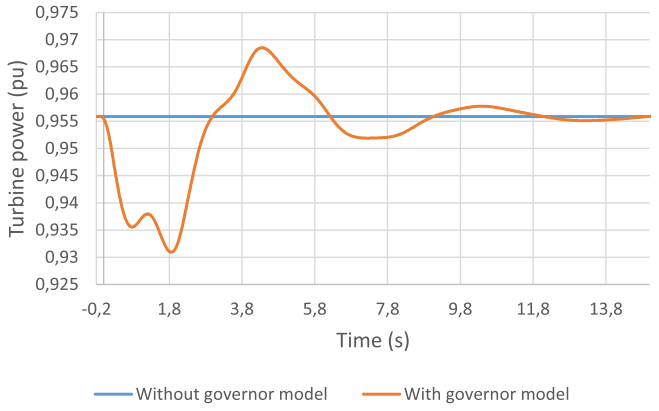

Fig. 5. Evolution of the generator 3 turbine power with and without a governor model regulation.

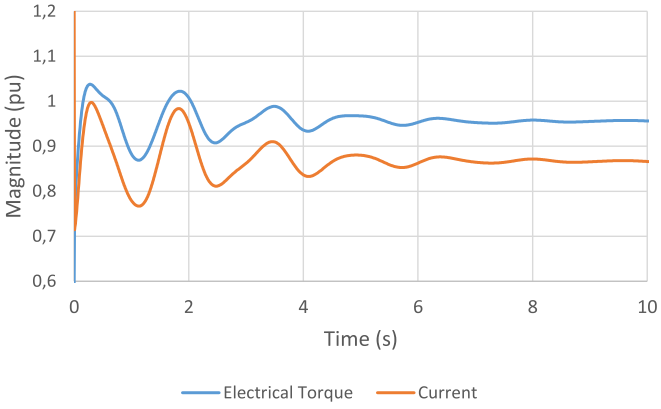

Fig. 6. Evolution of the electrical torque and the current of generator 3 after a short-circuit.

4 Impact of the modularization of one machine

4.1 Mechanical impact

A first impact of dividing one alternator into smaller turbo-generators is to split the kinetic energy and then the mechanical inertia in multiple parts. Knowing that the kinetic energy of a rotating mass is:

$$E_\mathrm{kin} = \frac{1}{2}J\Omega^2 \quad (2)$$

with

- J the moment of inertia of the generator and turbine (in kg m^2) and
- Ω the mechanical rotating speed (in rad s^{-1}).

The inertia constant H (related to nominal apparent power or nominal active power) of an alternator [15] can be defined as:

$$H_{S_\mathrm{n}} = \frac{E_\mathrm{kin}}{S_\mathrm{n}} \quad \text{or} \quad H_{P_\mathrm{n}} = \frac{E_\mathrm{kin}}{P_\mathrm{n}} \quad (3)$$

with S_n and P_n representing relatively the nominal apparent power and the nominal active power (in VA and W, respectively). The analysis of the impact of inertia constant is explained later, in parts 4.3 and 4.4.

4.2 Electrical impact

Although the considered short-circuit is not at the terminals of one machine in particular, two approaches based on this assumption will be drawn. This work aims at understanding which characteristics influence the behaviour of synchronous machines in case of short-circuit.

Indeed, the analyses presented below are not directly concerning frequency, but notions of current and electrical (resistive) torque are linked (see Fig. 6). As explained in equation (1), notions of frequency and electrical torque are indeed intrinsically related. Then, notions of frequency and short-circuit current (that fails feeding loads) are linked.

That is why understanding how, theoretically, the current evolves in a synchronous machine after a short-circuit event allows us to figure out general trends on the evolution of the frequency.

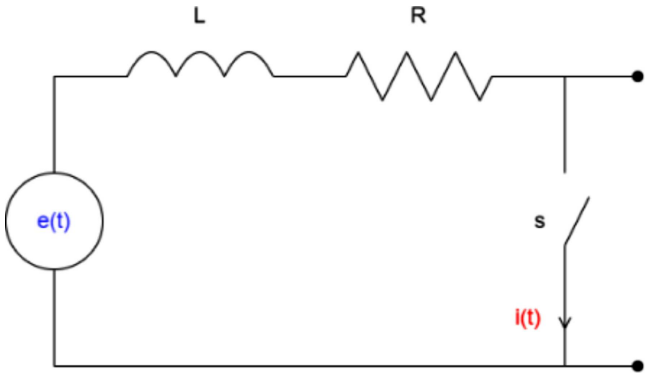

Fig. 7. Simple RL circuit with a switch to short-circuit.

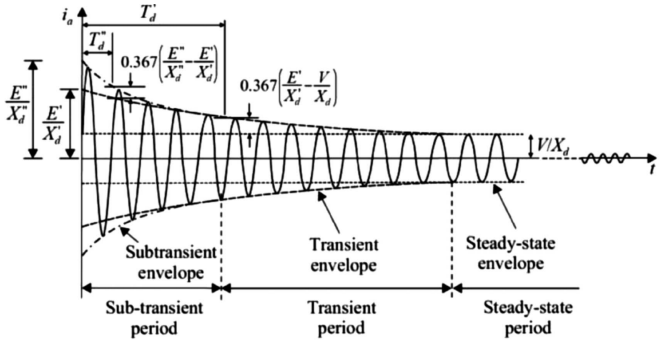

Fig. 8. Evolution of armature current during a short-circuit with a 6th order synchronous machine model [16].

4.2.1 Short-circuit with a Behn-Eschenburg model

Let us consider a simple RL circuit as shown in Figure 7, similar to a Behn-Eschenburg model of synchronous machine.

Kundur [15] explains that with a generator e such as:

$$e(t) = E.\sin(\omega t + \varphi) \tag{4}$$

when s is closed, the current is:

$$i(t) = \underbrace{\frac{E}{c_2}\sin(\omega t + \varphi - c_3)}_{\text{steady-state}} + \underbrace{c_1.e^{-\frac{R}{L}t}}_{\text{transient}}. \tag{5}$$

That means that the short-circuit has an alternating component (the steady state alternating signal) in an exponential decreasing envelope. This exponential part decreases with a time constant defined by R/L. The smaller the inductance L is, the faster the exponential decreases.

4.2.2 Short-circuit with a 6th-order model

For the sixth-order model used, an analysis of short-circuits [15,16] leads to a more complex but similar result. By neglecting some terms, equation (6) [18] shows the evolution of current in phase a of a three-phase machine after a short-circuit. The time constants that depend on the parameters of all circuits ($T_{\mathrm{d}}^{'}$ mainly depends on the rotor circuit, $T_{\mathrm{d}}^{'}$ on the damping direct-axis circuit, α on the stator circuit) drive the evolution of current after a short-circuit.

$$\begin{aligned} i_a(t) = -E\sqrt{2}\Bigg[& \underbrace{\frac{1}{X_d}}_{\text{steady-state}} + \underbrace{\left(\frac{1}{X_d^{'}} - \frac{1}{X_d}\right)\exp\left(-\frac{t}{T_d^{'}}\right)}_{\text{transient}} \\ & + \underbrace{\left(\frac{1}{X_d^{''}} - \frac{1}{X_d^{'}}\right)\exp\left(-\frac{t}{T_d^{''}}\right)}_{\text{subtransient}}\Bigg]\cos(\omega t + \varphi) \\ & + \underbrace{\frac{E\sqrt{2}}{2}\left(\frac{1}{X_d^{''}} + \frac{1}{X_q^{'}}\right)\exp(-\alpha t)\cos(\varphi)}_{\text{aperiodic term}}. \end{aligned} \tag{6}$$

And the smaller the time constants are, the faster the transient and subtransient end (see Fig. 8). The smaller the coefficients of the exponential are, the smaller the short-circuit current values are.

In tables of [19], synchronous inductances (x_{d}), transient inductances ($x_{\mathrm{d}}^{'}$), subtransient inductances ($x_{\mathrm{d}}^{''}$), transient open-circuit time constants ($T_{\mathrm{d0}}^{'}$) and subtransient open-circuit time constants ($T_{\mathrm{d0}}^{''}$) of typical nuclear units are provided. Knowing that the transient time constant and the subtransient time constant are, respectively, defined as [15,18]:

$$T_d^{'} = \frac{x_d^{'}}{x_d}T_{d0}^{'} \quad \text{and} \quad T_d^{''} = \frac{x_d^{''}}{x_d^{'}}T_{d0}^{''}. \tag{7}$$

Thus, similarly as inertia constants, it is possible to identify trends in the evolution of those parameters with the power of alternators. This is presented in part 4.3.

4.3 Input data

We do consider in this paper that the modularization of a nuclear power plant consists in replacing it by four SMRs. A literature review led to find various turbine-generator features in reference [19]. This is the most complete and exhaustive source of information found on this topic because all those data are often protected by industrial designers. This reference includes low power nuclear features that can be identified as SMR features, thus enabling us to adapt the grid production capacity accordingly to the proposed strategy.

Because rotors cannot be considered as cylinders whose radius increases with power, it is not true to consider that the moment of inertia quadratically increases with power. However, in Figure 9, typical inertia constants for nuclear units are displayed (dots) and also the inertia of the five-considered nuclear generators in the 39-bus grid (crosses). By extrapolating the trends suggested in Figure 9, it looks that the inertia (as previously defined) decreases when the nominal active (or apparent) power increases. That

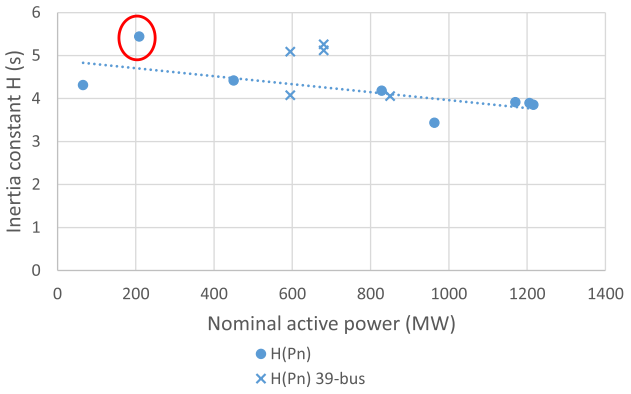

Fig. 9. Evolution of nuclear unit's inertia constants as a function of nominal active power in the 39-bus grid and according to [19].

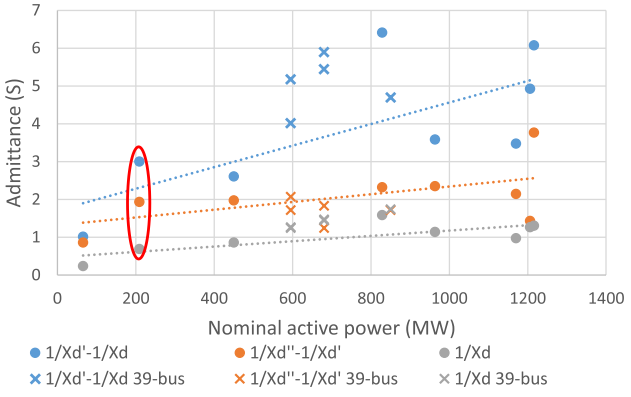

Fig. 10. Evolution of nuclear unit's admittance characteristics of short-circuit behaviour, as a function of nominal active power in the 39-bus grid and according to [19].

means the total inertia of small alternators should be more favourable than the inertia of larger alternator.

Figure 10 shows transient, subtransient and steady-state admittance coefficients from [19] and from the 39-bus grid and that are characteristics of short-circuit synchronous machine behaviour. Finally, Figure 11 shows transient and subtransient direct-axis time constants from [19] and from 39-bus grid.

From Figures 10 and 11, it appears that reducing the power of alternators reduces the coefficients and the time constants of the decreasing exponential of nuclear power units current. As analysed in 4.2, it would qualitatively explain why the frequency maximum is reduced. Then, modularizing power plants seems to be more favourable also from an electrical point of view, given the features found in [19].

The chosen SMR has a nominal apparent power of 245.5 MVA (or 208.25 MW) and its features are circled in red in Figures 9–11. More features of this SMR are given in Appendix A.

For this preliminary study, let us assume that the characteristics of the regulations (AVR, gov and PSS) do not depend on the SMRs but on the generator that is replaced.

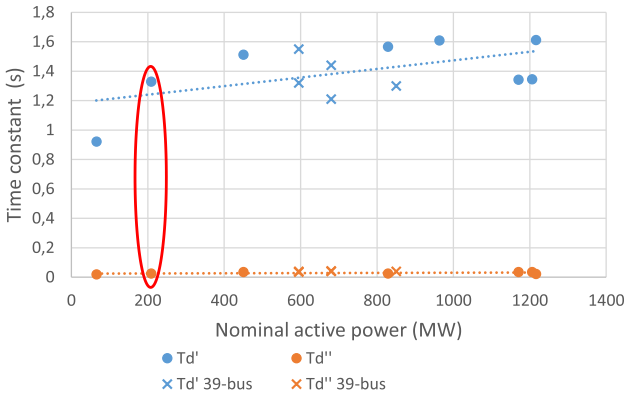

Fig. 11. Evolution of nuclear unit's transient and subtransient time constants as a function of nominal active power in the 39-bus grid and according to [19].

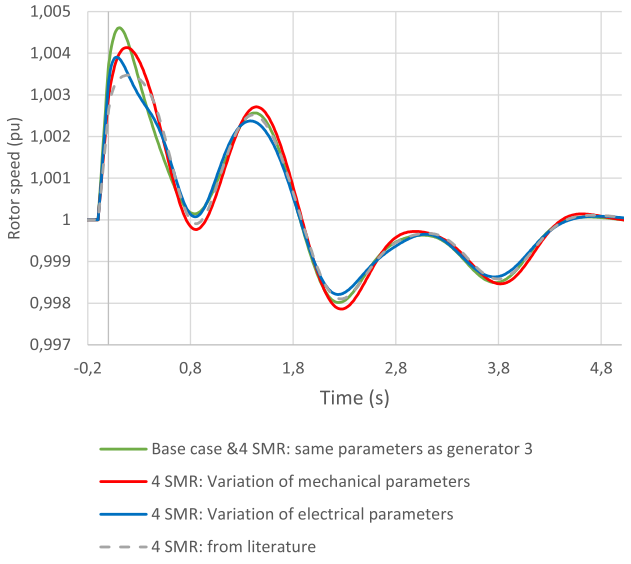

Fig. 12. Evolution of rotor speed with different machine set of parameters.

In other words, each SMR does take exactly the same regulations as the generator that it replaced.

4.4 Results

The impact of the modularization of generator 3 is presented in Figure 12. This figure presents the evolution of rotor speed of generator 3 and of one of the SMR replacing it after the short-circuit presented in part 2.5.

If modularization only consists in dividing generator 3 into four smaller generators with the same inertia constant, same electrical time constants and same inductances (in pu[1]), both of the simulations are exactly giving the same results, confirming the conclusion of the hypothesis in part 2.4. This result is the one represented by the green curve in Figure 12, representing both the base case

[1] In per-unit system, quantities are expressed as fractions of defined base unit quantity.

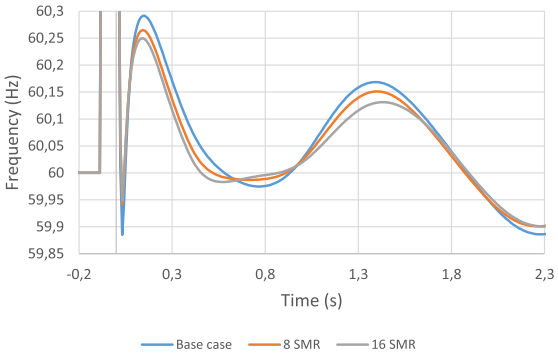

Fig. 13. Evolution of frequency at bus 19 with different number of SMR in the grid.

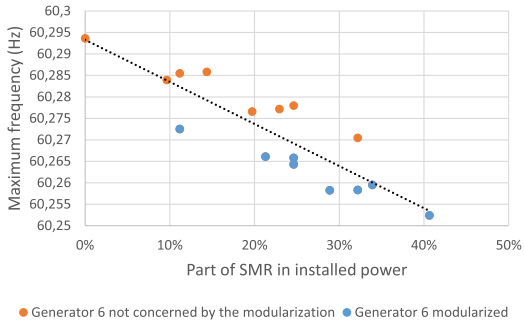

Fig. 14. Evolution of maximum frequency against the part of modularized installed capacity in the grid.

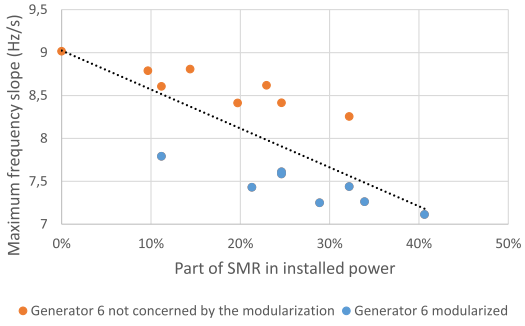

Fig. 15. Evolution of maximum frequency slope against the part of modularized installed capacity in the grid.

(without SMRs) and the case where 4 SMRs have strictly the same parameters than the large power machine. In this figure, the "variation of mechanical parameters" consists in taking into account only the variation of the mechanical parameters (moment of inertia (Eqs. (2) and (3)) without modifying their electrical parameters. Similarly, the "variation of electrical parameters" keeps the same mechanical parameters but takes into account the variation of time constants and inductances of the new SMR. The speed rotor of the SMR with all the parameters coming from the literature, both the mechanical and the electrical ones, is also presented in the grey dashed line.

It appears that taking into account only the mechanical parameters of smaller alternators, only the electrical parameters or both together always lead to reduce the maximum rotor speed (and thus the maximum frequency) and to smooth the variation of rotor speed after a short-circuit as explained in Sections 4.1 and 4.2.

5 Impact of the modularization of several reactors on the grid frequency

5.1 Input data

In this part, the modularization consists in replacing each of the generators 3, 6, 8 and 9 by four SMRs. Here also, the characteristics of the regulations are the same as the generator that is replaced. In total, there are 16 combinations of modularization, from no modularization to the four generators modularized. While considered as a nuclear power plant, no modularization of Generator 2 is carried out since it is the reference machine[2] of 39-bus grid.

Before assessing the three estimators presented in Section 3.1 for each new modularization, Figure 13 shows the evolution of the frequency at bus 19 (time origin is the end of short-circuit) in several configurations. Let us remind that "base case" is the initial 39-bus grid from the benchmark [13], without SMR. "8 SMR" is the 39-bus grid with generators 3 and 6 that are, respectively, replaced by four SMRs and "16 SMR" is the 39-bus grid with generators 3, 6, 8 and 9 that are all replaced by four SMRs.

As shown in Figure 13, it seems that modularizing has a positive impact on bus 19. Then, to generalize this result to the whole grid, it is useful to apply the three estimators that were previously defined.

5.2 Results

For each new modularization, the three estimators of frequency stability are calculated.

The results that are shown in Figure 14 represent the maximum frequency on the grid in function of the rate of modularized power plant versus the total capacity implemented on the grid. This means that the x-axis represents the sum of the SMR installed capacity divided by the sum of all the installed capacity on the 39-bus grid, except generator 10, which represents the interconnection. Figure 15 shows the maximum frequency slope on the grid against the rate of modularized power plant. In addition, Figure 16 shows the maximum of return times to $60\,\text{Hz} \pm 0.2\,\text{Hz}$ against the rate of modularized power plant. In the set of figures from Figures 14–16, the orange dots are the estimator results without generator 6 being

[2] "The reference machine, also called slack bus, in a load flow program must compensate for the gap between the power demand and the power supply by the other generators (nuclear, hydraulic and RES), taking into account the losses on the network. In reality, several machines adapt their production to avoid a possible overproduction/underproduction on the grid" [2].

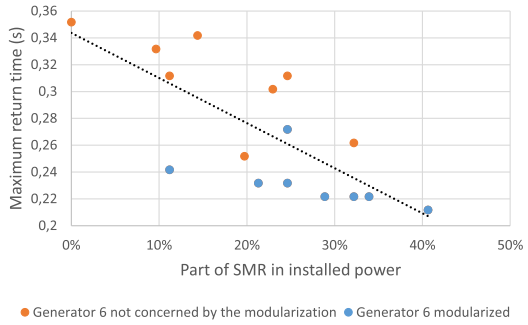

Fig. 16. Evolution of maximum return time against the part of modularized installed capacity in the grid.

Table 1. Estimator results for the extreme cases of modularization.

Number of SMRs	0	16	
Modularized generators	None	3, 6, 8, 9	
Part of SMR in installed capacity	0%	40.6%	
Maximum frequency (Hz)	60.294	60.252	↘−14.0%
Bus	19	20	
Maximum frequency slope (Hz/s)	9.0	7.11	↘−21.1%
Bus	19	19	
Maximum return time (s)	0.352	0.212	↘−39.8%
Bus	2	19	

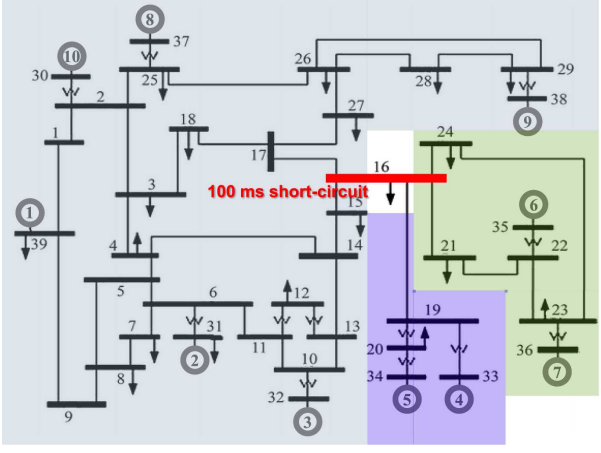

Fig. 17. Illustration of three zones next to the short-circuit bus [20].

modularized. The blue dots are then the results for which generator 6 is among the modularized generators.

The results show that for all three frequency stability estimators, the modularization has a positive impact. In this grid and for the fugitive short-circuit presented, when the modularized plant's installed power goes from 0% to 40%, the maximum frequency deviation decreases by 14% (see Tab. 1). As for the maximum frequency slope on the grid, the modularization of the four nuclear power plants previously listed leads to a 21% reduction of the slope. Finally, the results of the maximum return time are more scattered than for the two other estimators, but the trend shows a reduction of 40% by modularizing. Then, it appears that replacing big nuclear units by small nuclear units reduces the maximum frequency on the grid, smooths the worst frequency slope and accelerates the return to the final frequency.

Moreover, we can observe that another point seems to be important in the results as shown in Figures 14–16. It deals with the localization of the modularized power plants. Indeed, all results show that when Generator 6 is replaced by SMR, the estimators are smaller. Generator 6 is in the green area in Figure 17. That means that the distance to an event and the meshing of the network seems to have an influence as well in case of a short-circuit. To confirm this result in general cases, other types of event must be studied.

6 Conclusions

In the framework of energy transition, it is planned to increase the integration of non-dispatchable Variable Renewable Energies (VREs) and to reduce the rate of dispatchable fossil fuel power plants in the energy mix. One of the challenges is to keep the frequency, voltage and angular stability of the electrical network. Small Modular Reactors (SMR) could be an opportunity since they would be dispatchable, more geographically distributed and potentially more flexible for several reasons as discussed in the introduction.

This preliminary assessment aims to check if replacing large Nuclear Power Plants (NPPs) by SMRs could enhance frequency stability. To this end, the behaviour of the 39-bus grid electrical transmission network after a fugitive short-circuit has been simulated using a dynamic simulation software. Three estimators are used to quantify the frequency stability after this short-circuit: the maximum frequency on the grid, the maximum frequency slope on the grid and the maximum return time to a frequency of 60 ± 0.2 Hz.

It appears that for each of those estimators, modularization seems to have a positive impact. In the case of the presented event, the maximum frequency is reduced by 14%, the maximum frequency slope is reduced by 21% and the maximum return time is reduced about 40%. Thus, modularizing seems to enhance the frequency stability. Indeed, by extrapolating the analysis of the behaviour of one alternator after a short-circuit at its terminals, it is possible to explain how the mechanical and electrical parameters that are used to model the SMR are more favourable for the network behaviour concerning frequency stability.

To consolidate these results, other parameters should be used for the considered event and the performed study, especially the localization of the short-circuit or the parameters of the modularized generators that only come from one source. Moreover, other events should be taken into account to be more representative of the question of the impact of SMRs in the future power systems, as a load variation or a generation variation by modelling VREs on the 39-bus grid. Finally, to confirm the results and trends, it should be interesting to simulate all those kinds of events with other power systems.

Conflict of interests

The authors declare that they have no competing interests to report.

Funding

This research did not receive any specific funding.

Data availability statement

Data associated with this article cannot be disclosed.

Author contribution statement

All the authors were involved in the preparation of the manuscript. All the authors have read and approved the final manuscript.

Appendix A Parameters of the synchronous machines of 39-bus grid

Table A.1 contains the features of the 10 machines of 39-bus grid and the features of the replacing SMR. Tables A.2 and A.3 contain the features of the two governor model used. Table A.4 contains the AVR parameters. Table A.5 associated with Figure A.1 represents the features and the diagram of the used PSS.

Table A.1. Sixth-order synchronous machine model.

Unit $n°$	$S^{(*)}_{nominal}$ MVA	$V^{(*)}_{nominal}$ kV	H[Sgn] s	xd p.u.	xq p.u.	xd′ p.u.	xq′ p.u.	xd″ p.u.	xq″ p.u.	Td0′ s	Tq0′ s	Td0″ s	Tq0″ s	xl p.u.	rstr p.u.
1	10000	16.5	5	2	1.9	0.6	0.8	0.4	0.4	7	0.7	0.05	0.035	0.3	0
2	700	16.5	4.329	2.065	1.974	0.4879	1.19	0.35	0.35	6.56	1.5	0.05	0.035	0.245	0
3	800	16.5	4.475	1.996	1.896	0.4248	0.7008	0.36	0.36	5.7	1.5	0.05	0.035	0.2432	0
4	800	16.5	3.575	2.096	2.064	0.3488	1.328	0.28	0.28	5.69	1.5	0.05	0.035	0.236	0
5	300	16.5	4.333	2.01	1.86	0.396	0.498	0.267	0.267	5.4	0.44	0.05	0.035	0.162	0
6	800	16.5	4.35	2.032	1.928	0.4	0.6512	0.32	0.32	7.3	0.4	0.05	0.035	0.1792	0
7	700	16.5	3.771	2.065	2.044	0.343	1.302	0.308	0.308	5.66	1.5	0.05	0.035	0.2254	0
8	700	16.5	3.471	2.03	1.96	0.399	0.6377	0.315	0.315	6.7	0.41	0.05	0.035	0.196	0
9	1000	16.5	3.45	2.106	2.05	0.57	0.587	0.45	0.45	4.79	1.96	0.05	0.035	0.298	0
10	1000	16.5	4.2	1	0.69	0.31		0.25	0.25	10.2		0.05	0.035	0.125	0
SMR	245.5	14.4	4.624	1.71	1.63	0.32	0.51	0.21	0.21	7.1	0.38	0.038	0.073	0.125	0.0032

Notes. $^{(*)}$Base power and base voltage for the calculation of the per unit quantities. The power factor is 0.85 for all machines.

Table A.2. IEEEG1 governor model.

Unit $n°$	K	T1	T2	T3	K1	K2	T5	K3	K4	T6	K5	K6	T4	T7	K7	K8	PNhp	PNlp	Uc	Pmin	U0	Pmax
1–9 and replacing SMR	20	0.2	1	0.6	0.3	0	0.5	0.25	0	0.8	0.3	0	0.6	1	0.15	0	0	0	−0.3	0	0.3	1

Table A.3. IEEEG3 governor model.

Unit $n°$	Tg	Tp	Sigma	Delta	Tr	a11	a13	a21	a23	Tw	PN	Uc	Pmin	U0	Pmax
10	0.05	0.04	0.04	0.2	10	0.5	1	1.5	1	0.75	0	−0.1	0	0.1	1

Table A.4. EXST1 model.

Unit $n°$	Ka	Kc	Kf	Ta	Tb	Tc	Tf	Tr	Vimin	Vimax	Vrmin	Vrmax
All	200	0	0	0.015	10	1	1	0.01	−0.1	0.1	−5	5

Table A.5. Conventional Power System Stabilizer.

Unit $n°$	Kpss	Tw	T1	T2	T3	T4	Vmin	Vmax
1	1	10	5	0.6	3	0.5	−0.2	0.2
2	0.5	10	5	0.4	1	0.1	−0.2	0.2
3 and replacing SMR	0.5	10	3	0.2	2	0.2	−0.2	0.2
4	2	10	1	0.1	1	0.3	−0.2	0.2
5	1	10	1.5	0.2	1	0.1	−0.2	0.2
6 and replacing SMR	4	10	0.5	0.1	0.5	0.05	−0.2	0.2
7	7.5	10	0.2	0.02	0.5	0.1	−0.2	0.2
8 and replacing SMR	2	10	1	0.2	0.5	0.1	−0.2	0.2
9 and replacing SMR	2	10	1	0.5	2	0.1	−0.2	0.2
10	1	10	1	0.05	3	0.5	−0.2	0.2

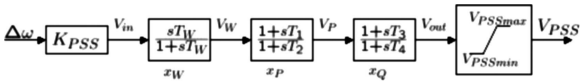

Fig. A.1. Representation of the used PSS [13].

Table B.1. Maximum difference of load flow results between Matlab-IEEE-Benchmark and PowerFactory load flows for each physical value.

Bus	Voltage (pu)	Angle (°)	Bus total P (MW)	Bus total Q (MVAr)	Load P (MW)	Load Q (MVAr)	Generator P (MW)	Generator Q (MVAr)	Unit $n°$
12	5×10^{-5}								
23					6×10^{-6}	6×10^{-6}			
31			−0.001				−0.001		2
34		−0.005							5
36								−0.005	7
39				0.019					1

Appendix B Comparison of load flow results from the IEEE benchmark and PowerFactory

Table B.1 presents for each column for 2 to 9, the greatest value associated with its bus (first column) and the generator (last column) if one is linked to.

References

1. International Energy Agency, *Status of Power System Transformation 2019: Power System Flexibility* (IEA, Paris, 2019)
2. A.-L. Mazauric, P. Sciora, V. Pascal, J.-B. Droin, Y. Besanger, N. Hadjsaïd, Q.-T. Tran, N. Guyonneau, Simplified approach to determine the requirements of a flexible nuclear reactor in power system with high insertion of variable renewable energy sources, EPJ Nucl. Sci. Technol. **8**, 5 (2022)
3. NEA; OECD, *Small Modular Reactors: Nuclear Energy Market Potential for Near-term Deployment* (OECD/NEA Publishing, Paris, 2016)
4. International Energy Agency, *Nuclear Power in a Clean Energy System* (IEA, Paris, 2019)
5. D. Michaelson, J. Jiang, et al., Review of integration of small modular reactors in renewable energy microgrids, Renew. Sustain. Energy Rev. **152** (2021)
6. B. Poudel R. Gokaraju, et al., Small Modular Reactor (SMR) based hybrid energy system for electricity & district heating, IEEE Trans. Energy Convers. **36**, 2794 (2021)
7. A. Sabir, D. Michaelson, J. Jiang, et al., Load-frequency control with multimodule small modular reactor configuration: Modeling and dynamic analysis, IEEE Trans. Nucl. Sci. **68**, 1367 (2021)
8. A.A.E. Abdelhameed, Y. Kim, et al., Three-dimensional simulation of passive frequency regulations in the soluble-boron-free SMR ATOM, Nucl. Eng. Design **361**, 2699 (2020)
9. International Atomic Energy Agency, Small Modular Reactors, [En ligne]. Available: https://www.iaea.org/topics/small-modular-reactors [Accessed 15 July 2021]
10. International Atomic Energy Agency, *Instrumentation and Control Systems for Advanced Small Modular Reactors* (IAEA Nuclear Energy Series, Vienna, 2017)
11. T. Athay, R. Podmore, S. Virmani, et al., A practical method for the direct analysis of transient stability, IEEE Trans. Power Appar. Syst. **PAS-98**, 573 (1979)
12. M.A. Pai, *Energy Function Analysis for Power System Stability* (Springer, New York, NY, 1989)
13. IEEE PES Task Force on Benchmark Systems for Stability Controls, Benchmark Systems for Small-Signal Stability Analysis and Control, [En ligne]. Available: http://www.sel.eesc.usp.br/ieee/ [Accessed 21 June 2021]
14. DigSILENT GmbH, DIgSILENT PowerFactory Version 2020 User Manual, Gomaringen (2020)
15. P. Kundur, *Power System Stability and Control* (McGraw-Hill, New York, 1994)
16. M. Eremia, M. Shahidehpour, et al., *Handbook of Electrical Power System Dynamics: Modeling, Stability, and Control* (Wiley, Hoboken, 2013)
17. G. Bhatt, S. Affijulla, et al., Analysis of large scale PV penetration impact on IEEE 39-bus power system, in *IEEE 58th International Scientific Conference on Power and Electrical Engineering of Riga Technical University (RTUCON)* (2017), pp. 1–6
18. P. Barret, Régimes transitoires des machines électriques tournantes, Techniques de l'ingénieur (1985)
19. P.M. Anderson, A.A. Fouad, et al., *Power System Control and Stability*, 2nd edn. (Wiley, Hoboken, 2002)
20. D. Wu, M. Javadi, J.N. Jiang, et al., Preliminary study of impact of reduced system inertia in a low-carbon power system, J. Modern Power Syst. Clean Energy **3**, 82 (2015)

Cite this article as: Charly Boudot, Jean-Baptiste Droin, Pierre Sciora, Yvon Besanger, Bruno Robisson, Anne-Laure Mazauric. Small Modular Reactor-based solutions to enhance grid reliability: Impact of modularization of large power plants on frequency stability, EPJ Nuclear Sci. Technol. **8**, 16 (2022)